

PAPER • OPEN ACCESS

Measurement of complex surfaces using precision coordinate measuring machine with Zernike algorithms

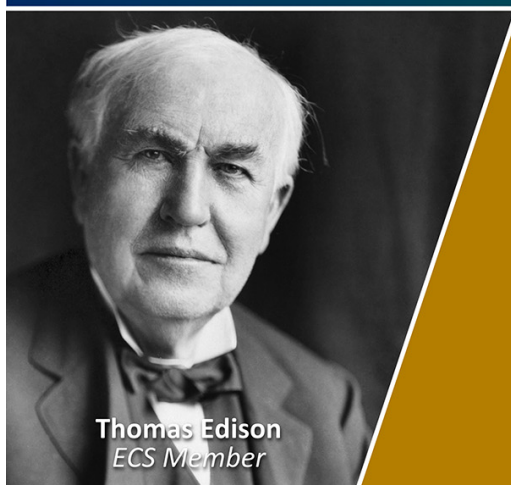
To cite this article: Juliana Mei yuk Tam *et al* 2025 *Meas. Sci. Technol.* **36** 065009

View the [article online](#) for updates and enhancements.

You may also like

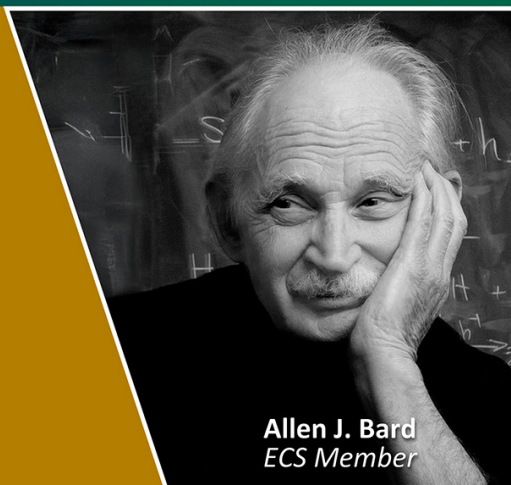
- [Pressure wave excitation and water pipeline leakage detection by using an air nozzle](#)
Li Wenlong, Zhao Linkun, Guo Xijian *et al.*
- [A review of rolling bearing fault diagnosis: data preprocessing and model optimization](#)
Wenlong Fu, Shuai Li, Bin Wen *et al.*
- [Construction of direct Z-scheme system for enhanced visible light photocatalytic activity based on \$Zn_{0.4}Cd_{0.3}S/FeWO_4\$ heterojunction](#)
Yunxiang Tang, Dezhi Kong, Xiaotong Wang *et al.*

Join the Society
Led by Scientists,
for *Scientists Like You!*



The
Electrochemical
Society

Advancing solid state &
electrochemical science & technology



Measurement of complex surfaces using precision coordinate measuring machine with Zernike algorithms

Juliana Mei yuk Tam^{1,2} , Henry Wong^{2,*}, Yixiao Han³, Gang Jin³ and Hester Chow⁴ 

¹ The State Key Laboratory of Intelligent Manufacturing Equipment and Technology, School of Mechanical Science and Engineering, Huazhong University of Science and Technology, Wuhan 430074, People's Republic of China

² Industrial Centre, The Hong Kong Polytechnic University, Hong Kong Special Administrative Region of China, People's Republic of China

³ Shanghai Institute of Technical Physics, Chinese Academy of Sciences, Shanghai, People's Republic of China

⁴ The HKPU, College of Professional and Continuing Education, Hong Kong Special Administrative Region of China, People's Republic of China

E-mail: icnswong@polyu.edu.hk

Received 25 July 2024, revised 7 May 2025

Accepted for publication 13 May 2025

Published 29 May 2025



CrossMark

Abstract

The paper introduces an innovative approach called Zernike-based CMM Surface Metrology (ZCSM) to enhance the accuracy of measuring large optical surfaces using coordinate measuring machines (CMMs). Traditional methods like laser interferometry and deflectometry, while precise, face limitations such as restricted dynamic range and sensitivity to specific surface properties. CMMs offer a promising alternative but are susceptible to systematic errors, particularly due to probe deflection when scanning, which can introduce geometric errors not present on the test surface. ZCSM addresses this challenge by fitting the surface form using Zernike polynomials, decomposing form errors into wavefront aberrations. A notable feature of the ZCSM method is the dual-parameter error compensation, which iteratively removes errors by correcting wavefront aberrations and verifying surface profiles until within the tolerance range. The feasibility of ZCSM was validated by measuring an astronomical mirror using a ZEISS XENOS CMM. The results showed that ZCSM's accuracy is comparable to interferometry, underscoring its potential as a viable alternative for precision metrology. The research indicates that ZCSM significantly improves the measurement accuracy of CMMs for large optical surfaces. Future research could focus on refining the method to eliminate higher-order residual aberrations and angular offsets, further enhancing its precision and applicability.

Keywords: surface metrology, Zernike polynomials, coordinate measuring machine, geometric errors, optical surface

* Author to whom any correspondence should be addressed.



Original content from this work may be used under the terms of the [Creative Commons Attribution 4.0 licence](https://creativecommons.org/licenses/by/4.0/). Any further distribution of this work must maintain attribution to the author(s) and the title of the work, journal citation and DOI.

1. Introduction

The demand for high-performance, miniaturized, and multi-functional optical systems has led to the use of complex surfaces to achieve specific performance and functionality, especially in astronomical equipment. These surfaces offer designers greater flexibility to correct aberrations and create compact designs with wider fields of view and lower f -numbers [1–3]. However, measuring these complex surfaces, especially those with steep slopes, poses significant challenges due to the need for high dynamic range in surface metrology.

Traditional methods like wavefront measurement interferometry (WMI) [4–6] have limitations in dynamic range, cost, and flexibility, often requiring computer-generated holograms (CGHs) for steep surfaces. CGHs can introduce additional errors and costs [7, 8], and defects in their manufacturing can lead to erroneous diffraction patterns, affecting measurement reliability.

Recent advancements in surface metrology aim to achieve higher accuracy, increased dynamic range, and the ability to measure complex surfaces without compensation optics like CGHs. These advancements can be categorized into sub-aperture stitching, structured light scanning, and precision coordinate profilometry.

- Sub-aperture stitching or multi-sensor systems measurement [9–12]: this involves measuring smaller sections (sub-apertures) of a large surface and stitching them together or combining different types of metrology sensors (e.g., optical, laser and tactile). These methods enhance dynamic range and versatility but require efficient algorithms to accurately align data [13] from different sub-apertures or sensors.
- Structured light scanning: techniques such as deflectometry [14] and confocal microscopy [15] offer non-contact surface testing methods [16] that do not require CGHs. Confocal microscopy provides high-resolution measurements by focusing light to a very small spot on the surface, while deflectometry based on triangulation principles measures surface profile with sub-nanometer precision in synchrotron mirror metrology applications [17]. These methods are particularly useful for measuring reflective surfaces but require rigorous calibration to ensure accurate measurements, especially for low-order aberrations. However, they still face challenges with line-of-sight issues and slope-ambiguity, and less feasible for complex surfaces.
- Precision coordinate profilometry: coordinate measurement machines (CMMs) [18–21] and stylus profilometers are used for high-precision geometric dimensioning and tolerance measurements, achieving micron-level accuracy. Stylus profilometers [22–25] are widely used to measure surface roughness and texture but have limited movement range, making them less suitable for large surface measurements [22]. Therefore, Yang and Peng have developed a stitching method to extend the measurement coverage for measuring large aperture mirrors [23].

CMMs are suitable for large surfaces due to their flexibility and high dynamic range. In 2005 [26], Li and Gu demonstrated the capability of CMMs for measuring complex surfaces with micron-level accuracy. CMMs have been widely researched and applied in various fields, including optical surface measurement [21], large surface on-machine measurement [25] and swing arm profile measurement [27].

Tactile CMMs operate by physically probing points on a surface and recording their position relative to a reference coordinate system, are therefore susceptible to systematic errors in the measurement process. Accurate alignment is crucial for reliable measurements, as any probe arm flexure will introduce systematic geometric errors. Especially for large complex surfaces, those with gentle curves (large radii), even small deflections can lead to significant errors. Astronomical mirrors, which often have large radii of curvature, are particularly susceptible to these structural drifts. Therefore, the manufacturing accuracy of the large spaceborne mirror is often limited by measurement errors [28]. Therefore, methods are needed to offset systematic errors and improve the measurement accuracy of CMMs for large and complex surfaces.

Various methods have been proposed to mitigate misalignment errors in CMM measurements, including feature-based alignment and mathematical methods based on deviations analysis.

Feature-based alignment utilizes geometric feature [29] or fiducial-aided markers [30] as reference points for alignment. These methods are effective for parts with unique features such as holes and edges, but may not be suitable for featureless or finely detailed optical surfaces. Additionally, placing artificial fiducials on optical surfaces can be challenging and may introduce additional errors or damage the surface.

Mathematical methods are based on analyzing the deviation from a [26] using specifically defined parameters (e.g. radius of curvature or distance), reducing reliance on invariant features or fiducial aids. Although these methods are widely used, they require sophisticated algorithms and are computationally intensive.

Zernike polynomials [31] are widely used in optical surface metrology to decompose the surface form error into a series of wavefront aberrations. They provide a systematic approach to identifying and eliminating false aberrations. Errors due to misalignment typically introduce low-order aberrations in the Zernike polynomials. However, the effectiveness of the error correction depends on the accuracy of the Zernike fit and the ability to identify the relevant aberrations. Therefore, effective compensation strategy is important to ensure the geometric errors that not actually present on the test surface are eliminated.

Currently, WMIs, such as laser interferometers [5–8], are often used in complex surface precision metrology research to provide higher accuracy. However, these methods are constrained by their limited dynamic range and sensitivity to certain surface properties. Furthermore, a high-cost CGH is required to ensure a self-collimating light path. CMMs, especially ultra-precision models like the ZEISS XENOS, are

emerging as powerful tools for precision metrology, offering sub-micron accuracy, high point density, and a wider dynamic range. However, existing studies, such as that of Wang *et al*, using a CMM with probe radius compensation [21], did not fully address the systematic measurement error caused by the probe deflection under tactile scanning, which can significantly affect the measurement accuracy.

The paper proposes a novel approach called Zernike-based CMM Surface Metrology (ZCSM) to address these challenges of measuring large optical surfaces. This method leverages Zernike polynomials to fit the surface form error and decompose the geometric error through wavefront aberrations. A key component of the ZCSM is the dual-parameter error compensation (DEC) model, which iteratively compensates for erroneous geometric errors that are not actually present on the test surface. This combination counteracts systematic errors caused by probe deflection when scanning large, gently curved surfaces. The ZCSM framework consists of several key steps: data acquisition, outlier removal and high frequency noise filtering, Zernike fitting, wavefront aberration correction and reconstructed profile verification.

The effectiveness of the ZCSM method is demonstrated through experiments conducted on an astronomical mirror using an ultra-precision CMM. The results are compared with those obtained using a commercial WMI, showcasing the potential of ZCSM as a reliable alternative for precision metrology of large optical surface measurements.

The paper is structured as follows: Chapter 2 introduces the framework of ZCSM. Chapter 3 details the data acquisition process. Chapter 4 describes the outlier elimination and Gaussian filtering used in the study. Chapter 5 introduces surface fitting using Zernike polynomials. Chapter 6 elaborates on the DEC Compensation Model. The experiments and results are discussed in chapter 7. Finally, chapter 8 provides the conclusion.

2. Framework of ZCSM

The ZCSM is introduced to address the challenges of measuring large mirrors, particularly the geometric uncertainties introduced by probe deflection when tactile scanning is performed using a CMM. The framework of ZCSM, illustrated in figure 1, is a comprehensive approach designed to enhance the accuracy of measuring large and complex surfaces, such as astronomical mirrors. It integrates advanced data acquisition and pre-processing techniques, Zernike fitting and DEC compensation strategies to ensure precise surface form measurements.

The data acquisition process starts with measurement path generation. This process determines the measuring pattern for the CMM to ensure complete surface coverage, configures measurement parameters for the specific surface being measured, and automatically establishes measurement paths to streamline the process and increase efficiency.

To ensure the reliability of the data, the acquired data points are fitted to a best fit sphere (BFS) by the least square method, thus establishing a baseline for outlier elimination. A Gaussian

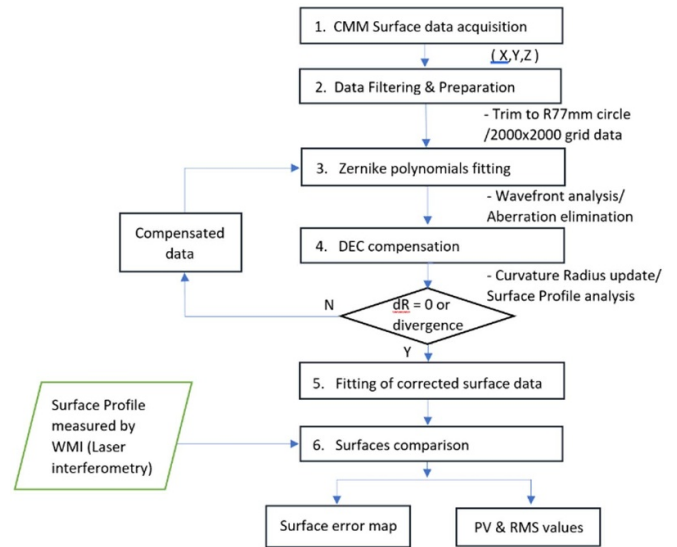


Figure 1. Framework of the ZCSM for measuring complex surface.

filter is applied to remove high frequency noise. The filtered data were processed into a uniformly distributed grid array for further comparison.

Zernike polynomials are used to fit the processed data, to effectively decompose the form error of optical surface into wavefront aberration. DEC is used to relate surface profile errors with wavefront aberrations to iteratively eliminate systematic geometric errors, including wavefront aberrations correction, surface error verification (i.e. decenter error (dR) analysis). Wavefront aberrations correction based on comparison of Zernike coefficients with WMI measurements to identify and subtract spurious geometric errors.

DR verification is to identify deflection-induced errors by comparing the surface radius of the BFS with the measured aspheric wavefront. Iterative verification involves repeatedly updating the surface radius and calculating the dR until the remaining different between the wavefront aberration and the geometric error is within the desired tolerance.

Finally, the surface was reconstructed using the corrected data and then compared with the measurements from the WMI to verify accuracy. Final results include error maps and quantitative values of the measured surface, which are exported for further analysis or reporting.

2.1. Aspheric surface

Aspheric surfaces are commonly used in optics to design lenses and mirrors that deviate from simple spherical shapes. The profile of an aspheric surface can be mathematically described by the following equation involving a conic part and a power series [31–33] :

$$z(x,y) = \frac{c(x^2 + y^2)}{1 + \sqrt{1 - (1+k)(x^2 + y^2)c^2}} + \sum_{i=2}^n A_{2i} \cdot (x^2 + y^2)^i \quad (1)$$

where z is the sagitta, which is the height of the surface perpendicular to the Z -axis; c is the curvature of the base sphere, defined as $c = 1/R$, where R is the radius of curvature; k is the conic constant, which determines the shape of the conic section; A_{2i} is the aspheric coefficients, corresponds to a term in the power series that adjusts the surface profile to achieve the desired aspheric shape.

2.2. BFS

BFS is an important concept in the analysis and fitting of aspheric surfaces. It provides a baseline reference that approximates the overall shape of the aspheric surface, making it easier to analyze and manipulate surface quantities.

BFS provides a simple, linear reference that helps to simplify the nonlinearities inherent in aspheric fitting. By approximating the surface with a sphere, it becomes easier to handle mathematically. During data processing, BFS can be used as a baseline to filter out noise from the measured data. Deviations from the BFS can be analyzed to understand the true shape of the asphere. For surface evaluation, BFS provides a quick and intuitive way to evaluate aspheres by providing a reference radius of curvature.

The algorithm for finding BFS involves minimizing the sum of the squared differences between the distances from the data points on the aspheric surface to the center of the sphere and the radius R . The mathematical expression can be expressed as follows:

$$\min_{a,b,c,R} \sum_{i=1}^N \left(\sqrt{(x_i - a)^2 + (y_i - b)^2 + (z_i - c)^2} - R \right)^2 \quad (2)$$

where R is the radius of the BFS; (x_i, y_i, z_i) are the coordinate of the data points on the aspheric surface; (a, b, c) represent the center of the BFS in the machine coordinate system.

To solve this minimization problem, various optimization techniques can be used, among which the least squares fitting is one of the most common used methods.

3. Data acquisition

Tactile precision CMMs are an effective tool for obtaining accurate surface data, especially for large and complex surfaces like astronomical mirrors. The measurement process of CMMs involves several steps: part alignment, measurement path planning and data sampling. Proper alignment of parts is crucial to minimizing systematic errors. The surface must be correctly positioned relative to the CMM's coordinate system to ensure accurate measurements. This step involves aligning the part so that its features are properly positioned relative to the machine's axes. For large, gently curved surfaces, a circular measurement path is often used. As shown in figure 2, the surface is divided into several concentric circles with different radii to ensure uniform data collection. This systematic approach helps to fully cover the entire surface.

The sampling process consists of measuring data points along a circular path radially along the test surface. After completing the measurement of one cross section, the CMM moves

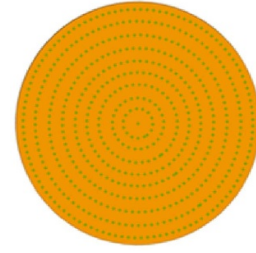


Figure 2. Concentric circular measurement pattern.

along the X -axis to the next section. This ensures that uniform data collection across the entire surface.

When scanning complex surfaces, especially those with gentle curves and large radii, it is crucial to minimize any potential errors introduced by the scan head such as probe arm flexure. Astronomical mirrors are particularly sensitive to structural drifts due to their large radius of curvature. Even a small deflection of the probe can lead to significant systematic errors that can seriously affect the measurement accuracy.

4. Outlier elimination and Gaussian filtering

Data filtering and pre-processing is critical to ensure that the data collected by a CMM accurately represents the surface geometry without interference from measurement noise and high frequency data, and to prepare the data for comparison with the WMI. Here's an outline of the steps involved:

- (1) Outlier elimination: erroneous data points caused by measurement errors that can affect the accuracy of surface fitting [27, 28, 34]. Outliers are first removed so that they will not influence the filtering step. This is done by fitting the data to BFS. Statistical thresholds are used to exclude anomalies. For data points from the single point probing sampling method, the errors are more random and usually follow a Gaussian distribution, with a 2-sigma applied, meaning that data points that are two standard deviations from beyond the fitted mean are considered outliers. From our experiment, continuous scans will introduce more systematic errors or correlated noise, which may not follow a perfect Gaussian distribution. A wider threshold, is used to avoid removing valid data points that may be part of the actual surface features. The threshold value depends on the data acquisition method. In this study, a sigma of 10 was used.
- (2) Gaussian filtering: CMM scanning captures both low-frequency form errors and high-frequency details of the surface. To smooth high frequency noise (small-scale roughness), while preserving low-frequency form error (large-scale shape deviations). Gaussian filters are applied by convolving the data with a Gaussian kernel. The Gaussian kernel $G(x, y)$ is given by:

$$G(x, y) = \frac{1}{2\pi\delta^2} e^{-\frac{x^2+y^2}{2\delta^2}} \quad (3)$$

where σ is the standard deviation, controls the length of the Gaussian filter curve.

The standard deviation determines the amount of smoothing. A larger σ results in a smoother effect, while a smaller σ preserves more high-frequency details. The filter length (i.e. standard deviation) should be chosen to be consistent with the spatial characteristics of the form error to ensure effective smoothing of high-frequency details.

- (3) Data processing: the filtered points are processed for further analysis. Boundary integrity and uniform data distribution are critical for data comparison. Boundary effects that can skew the analysis due to insufficient neighborhood data at the edges. A linear extrapolation padding is used to add data points based on the trends of nearby points. To facilitate comparisons across different measurement systems, a smaller aperture size was used in order to match the largest common diameter of different measurements (e.g. a circle with a radius of 77 mm) to focus on the common surface data, and reduce the impact of edge artifacts. To reduce the influence of the different data distributions between measurement systems, the data were interpolated into a regular 2000×2000 grid format. This also avoids errors due to sparse or uneven data distribution, thus facilitating more accurate and reliable analysis.

These steps are essential to making CMM data less susceptible to surface roughness and anomalies during surface evaluation. By effectively reducing the influence of boundary effects and differently distributed data between systems, the comparison results are more reliable and consistent. This integrated approach enhances the accuracy of surface analysis and comparison, especially for large complex surfaces like astronomical mirrors.

5. Surface fitting using Zernike polynomials

5.1. Zernike polynomials

Zernike polynomials are mathematical functions used to represent wavefront aberrations over a circular domain. They are particularly useful in optics to decompose surface form errors into a series of aberrations. In the ZCSM method, these polynomials help to identify and compensate for misalignment errors such as probe deflection, which can introduce low-order aberrations in the Zernike fit.

Zernike polynomials for a circular aperture are expressed as products of normalization factors, radial polynomials, and azimuthal (angular) functions [31, 32, 35],

$$Z_n^m(\rho, \theta) = \begin{cases} \sqrt{2(n+1)} R_n^m(\rho) \cos(m\theta), & m \geq 0 \\ \sqrt{2(n+1)} R_n^m(\rho) \sin(m\theta), & m < 0 \\ \sqrt{(n+1)} R_n^0(\rho), & m = 0 \end{cases} \quad (4)$$

where n is the degree of the radial polynomials; m is the azimuthal frequency describing the repetition of the angular function. Both n and m are non-negative integers satisfying $n - m \geq 0$ and $n - m$ is even.

The radial polynomial $R_n^m(\rho)$ is defined as:

$$R_n^m(\rho) = \sum_{k=0}^{\frac{n-m}{2}} \frac{(-1)^k (n-k)!}{k! \left(\frac{n+m}{2} - k\right)! \left(\frac{n-m}{2} - k\right)!} \rho^{n-2k}. \quad (5)$$

5.2. Wavefront fitting

The wavefront fitting process aims to eliminate geometric errors and accurately describe the surface profile of a test mirror measured by the CMM. This involves several steps:

- (1) Baseline preparation: the sampling points are fitted using the least squares method to obtain a BFS that approximates the surface. This BFS is processed into the same regular grid format as the gridded CMM dataset.
- (2) Wavefront deviation calculation: the wavefront deviations from the BFS are calculated by subtracting the 'BFS gridded dataset' from the 'CMM gridded dataset'. This represents the original wavefront of the CMM data.

$$\Delta W = Z_{\text{CMM}} - Z_{\text{BFS}} \quad (6)$$

where ΔW is the wavefront deviation, Z_{CMM} is the CMM gridded dataset, Z_{BFS} is the BFS gridded dataset.

- (3) Zernike polynomial fitting:

The sampling points (x, y, z) in Cartesian coordinates from CMM can be converted to polar coordinates (ρ, θ, z) and normalized by:

$$\rho = \sqrt{(x^2 + y^2)}/r \quad (7)$$

$$\theta = \tan^{-1}(y/x) \quad (8)$$

where r is the radius of the circular aperture.

The wavefront deviations are fitted using Zernike polynomials to describe optical aberrations,

$$\Delta W(\rho, \theta) = \sum_{n=0}^N a_n Z_n^m(\rho, \theta) \quad (9)$$

where a_n are the Zernike coefficients, Z_n^m are the Zernike polynomials, and N is the total number of Zernike polynomials in the expansion.

The ZCSM method fits the surface data to Zernike polynomials and identifies form errors that are not actually present on the test surface through wavefront aberrations comparison. This method can quickly and effectively eliminate systematic geometric errors, making CMM measurements of complex surfaces more accurate and reliable.

6. DEC compensation model

The DEC model is an advanced iterative approach designed to improve the accuracy of aspheric surface measurements by compensating for geometric errors. Error compensation is performed by systematically correlating the wavefront aberrations with the geometrical errors (radius of curvature) to ensure the true surface profile is retrieved.

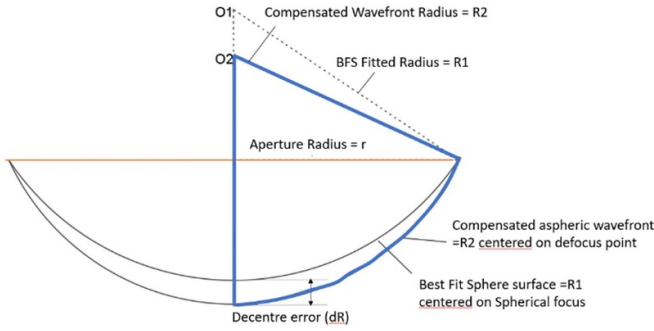


Figure 3. Schematic diagram of decenter error.

6.1. Surface profile error analysis

During the manufacturing process, a spherical surface is often used as a starting point for creating an aspherical surface because its radius of curvature very close to the radius of curvature of the intended aspherical surface. This minimizes material removal and enhances efficiency. The BFS is used to approximate the aspheric surface and the geometrical error is determined by measuring the difference between the BFS and the aspheric surface.

The dR is introduced to evaluate the measurement accuracy based on the analysis of curvature radius as shown in figure 3. This quantifies the deviation of the asphere from the ideal position of the BFS. This metric evaluates measurement accuracy by comparing the BFS spherical vertex (centered on the spherical focus, O_1) and the compensated aspheric wavefront (centered at the defocus point, O_2).

The dR can be described as follow:

$$dR = \left(R_2 - \sqrt{R_2^2 - r^2} \right) - \left(R_1 - \sqrt{R_1^2 - r^2} \right) \quad (10)$$

where R_1 is the radius of the fitted BFS, R_2 is the radius of measured aspheric wavefront and r is the aperture radius.

As shown in figure 3, the surface profile error is evaluated by assuming that the radius of the aspheric surface (compensated aspherical wavefront) and its fitted spherical surface (BFS) should be very close or equal. Geometric errors may result in radius deviations, which in turn lead to vertex shift and decenter offsets.

6.2. Wavefront error analysis

Zernike polynomials are used to decompose the surface form error into a series of wavefront aberrations, which helps to identify systematic geometric errors. The wavefront can be expressed as:

$$W(\rho, \theta)_{\text{measured}} = a_0 Z_0(\rho, \theta) + a_1 Z_1(\rho, \theta) + a_2 Z_2(\rho, \theta) + a_3 Z_3(\rho, \theta) + \dots, \quad (11)$$

where a_0 , a_1 , a_2 , and a_3 represent the coefficients of the piston, x -tilt, y -tilt, and defocus terms of the Zernike series, respectively.

Systematic geometric errors are detected by comparing Zernike coefficients of the WMI and subtracted by setting the low-order Zernike coefficients (piston, x -tilt, y -tilt, and defocus) to zero. The remaining aberrations after correction are then used to reconstruct the surface and determine whether further correction is needed.

6.3. Iterative error elimination

The DEC model employs an iterative process to refine the BFS curvature radius and wavefront aberrations. This involves correcting wavefront aberration of the measured surface, updating the BFS curvature radius based on corrected data, and calculating the dR to assess the accuracy of the correction.

The process continues until the value of dR is minimized, a predetermined threshold or maximum number of iterations is reached. After convergence, the DEC model provides the optimal radius value and the true surface form error for the aspheric surface, thereby eliminating the systematic geometric error.

The DEC model is crucial for high precision metrology applications, such as measuring high-performance mirrors in astronomical equipment. By systematically eliminating systematic geometric errors, the true surface profile of the asphere is restored.

In short, the DEC model is a comprehensive approach that combines surface profile error analysis, wavefront error analysis, and iterative error elimination to achieve high accuracy in aspheric surface measurement.

7. Experimental and results

The experiments conducted at the Shanghai Institute of Technical Physics of the Chinese Academy of Sciences aimed to evaluate the effectiveness of the ZCSM method in improving the measurement accuracy of large and complex optical surfaces.

The test sample is the astronomical mirror from the FengYun series of Chinese meteorological satellites, it is a weak aspherical mirror with a diameter of 190.8 mm and a radius of curvature of 1429.5 mm as shown in figure 4.

Two primary instruments were used: the XENOS CMM from Carl Zeiss and the PhaseCam 6000 interferometer from 4D Technology. The Zeiss CMM is known for high precision. Its measuring range is 900 mm × 1500 mm × 700 mm and its measuring accuracy of 0.3 μm, as shown in figure 5(a). The PhaseCam 6000 interferometer is a WMI with high measurement accuracy of 2% of the wavelength (632.8 nm), serving as a reference for comparison. The system layout is as shown in figure 5(b).

The measurements were conducted in a temperature-controlled room at 20 ± 0.2 °C and the CMM sampled data points along concentric circular paths as shown figure 2, moving along the X -axis for comprehensive coverage of the test surface. Outliers and high frequency data were filtered out, and BFS fitting was performed using the least square method on

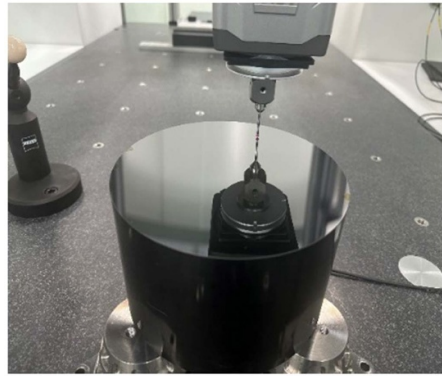
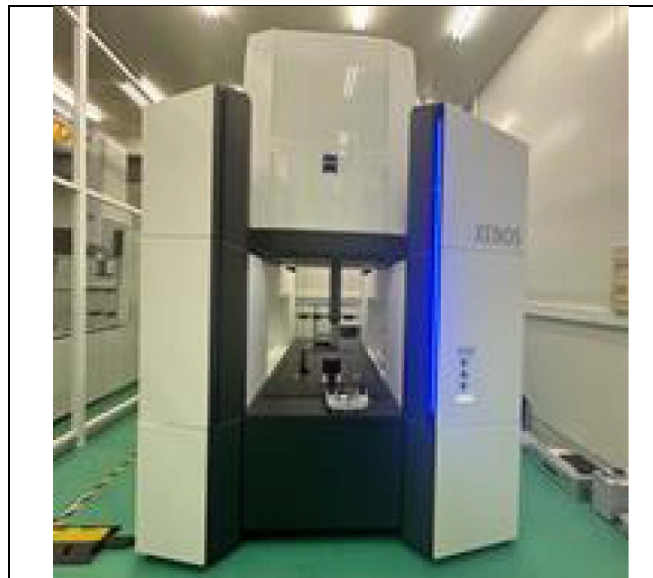
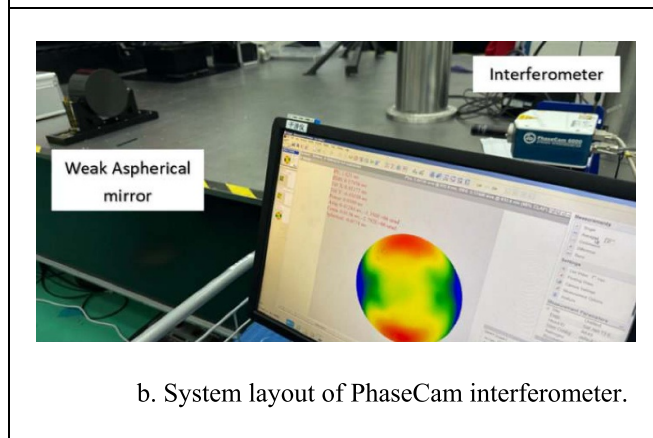


Figure 4. Test sample—astronomical mirror.



a. Testing mirror with Zeiss XENOS CMM.



b. System layout of PhaseCam interferometer.

Figure 5. (a) Testing mirror with Zeiss XENOS CMM. (b) System layout of PhaseCam interferometer.

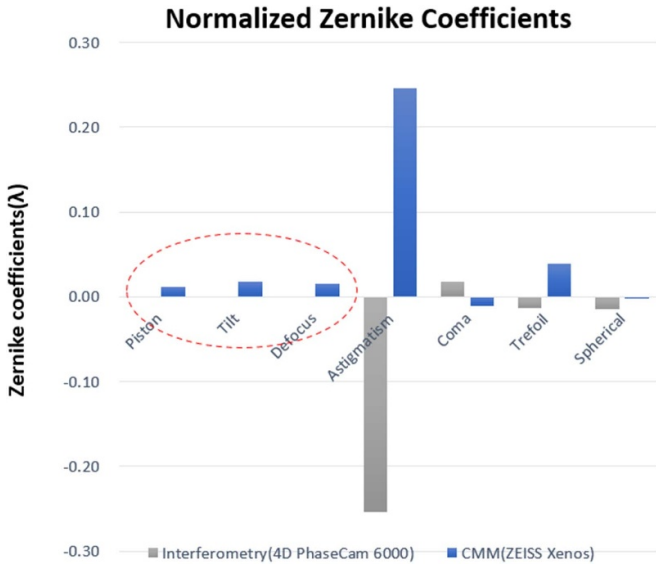


Figure 6. Comparison of Zernike coefficients in the measuring of an astronomical mirror surface.

the data as a reference surface. The fitting parameters in the equation (2) are:

$$\begin{aligned}
 r &= 1430.012\ 060\ 355\ 824\ \text{mm} \\
 a &= -0.089\ 539\ 004\ 573\ 845\ 24\ \text{mm} \\
 b &= 1.053\ 287\ 791\ 741\ 585\ \text{mm} \\
 c &= 1430.014\ 827\ 918\ 3775\ \text{mm}
 \end{aligned}$$

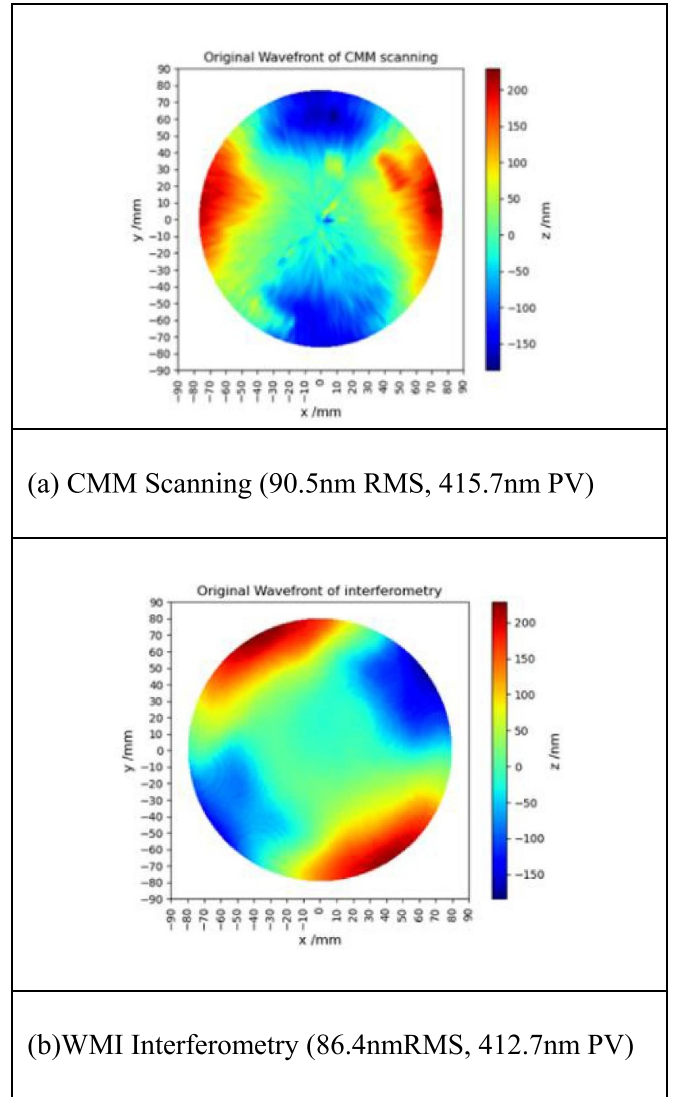
ZCSM is used to eliminate systematic measurement errors. A 36-term Zernike polynomial was used to decompose the surface form errors into wavefront aberrations. The DEC model is designed to iteratively correct wavefront aberrations and verify reconstructed surface profiles.

The coefficients of Zernike fit from both WMI and CMM measurements were compared in figure 6. The WMI data exhibited fewer geometric aberrations. The presence of spurious low-order aberrations, such as piston, tilt and defocus in CMM data, which are absent in the WMI results. This indicates that misalignment (e.g. probe arm flexure) are introducing geometric errors in the CMM data that are not actually present on the test surface.

The observed discrepancies in astigmatism measurements between the CMM and WMI in figure 6 can be attributed to the method-specific systematic errors and geometric misalignment.

Method-specific systematic errors: CMMs are susceptible to mechanical instabilities and can introduce structural drifts like astigmatism during prolonged measurements. WMIs are highly sensitive to environmental noise. Air turbulence, temperature fluctuations and vibrations can distort the interferogram, introduce high-frequency noise that alias into low-order terms, resulting in incorrect astigmatism.

Geometric misalignment: improper mirror positioning during setup (e.g. Misalignment of test mirrors) can introduce artificial astigmatism. Any angular or positional offsets between WMI and CMM setups can distort the measurement results, causing discrepancies between the two systems.



(a) CMM Scanning (90.5nm RMS, 415.7nm PV)

(b)WMI Interferometry (86.4nmRMS, 412.7nm PV)

Figure 7. Original measurement results of a test surface obtained with (a) Zeiss XENOS CMM (b) PhaseCam 6000 interferometry.

A combination of method-specific errors and geometric misalignment lead to divergent astigmatism values between the two methods. CMM errors (mechanical drift) and WMI error (environmental noise, aliasing) propagate differently into astigmatism calculations. Geometric misalignment can exacerbate discrepancies by introducing systematic offsets that are unique to each setting.

According to the quantitative results, CMM (Baseline) measurements yielded a root mean square (RMS) of 90.5 nm and a peak to valley (PV) of 415.7 nm, while WMI measurements showed an RMS of 86.4 nm and a PV of 412.7 nm. The CMM showed higher error value, indicating susceptibility to systematic geometric error. From qualitative observations in figure 7, the error map indicated the presence of ‘chatter’ in the CMM data, suggesting mechanical instability or contamination (e.g. dust on the stylus) during the scanning process.

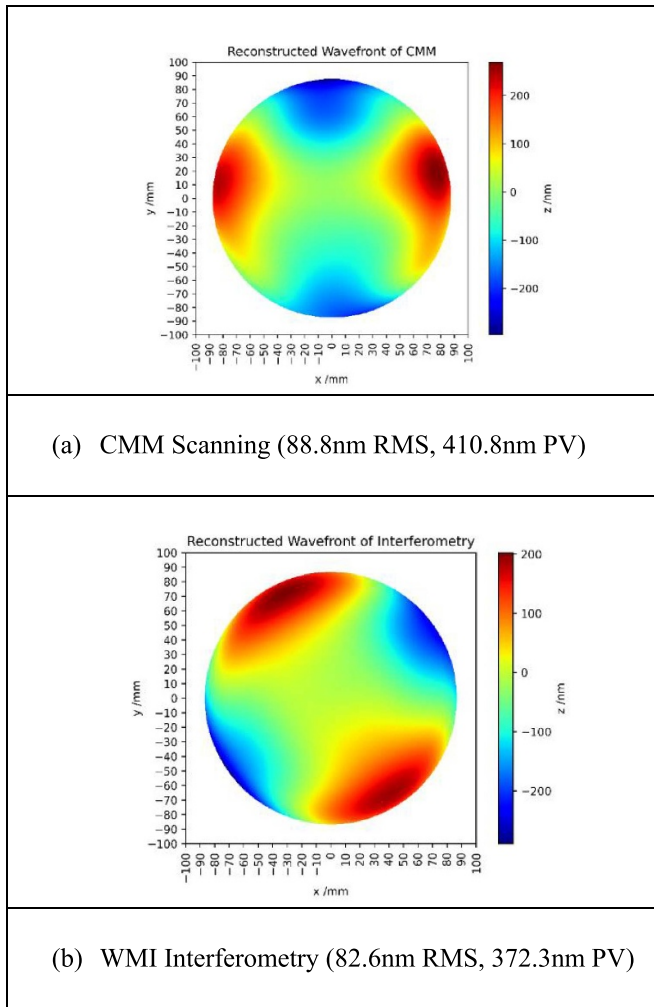


Figure 8. Measurement results obtained with (a) CMM-measured ZCSM method (b) WMI interferometry.

An obvious angular offset in the error maps between CMM and WMI measurements suggested discrepancies in the measurement setup, and that the test surface was oriented differently during each measurement.

In figure 8, the CMM with the ZCSM method yielded improved results: an RMS of 88.8 nm and a PV of 410.8 nm. The WMI measurements showed an RMS is 82.6 nm and a PV is 372.3 nm, which showed that the ZCSM method improves the accuracy of CMM measurement and reduces the systematic measurement error, aligning more closely with WMI measurements.

In figure 9, the comparison of Zernike coefficients revealed that the ZCSM method improves the CMM result, however residual aberrations remained, which indicates that further refinements are needed to eliminate higher-order background aberrations (e.g. astigmatism) and address angular offset issues.

Overall, the experiments demonstrated that the ZCSM method enhances the accuracy of CMM measurements for large complex optical surfaces, though further work is needed to address remaining challenges.

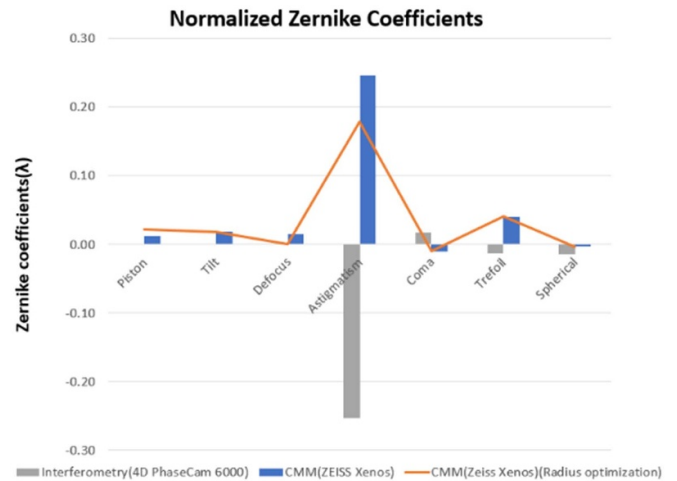


Figure 9. Comparison of Zernike coefficients in the testing of an astronomical mirror surface with CMM, CMM-measured ZCSM method and WMI.

8. Conclusion

The conclusion of the paper highlights the successful development and evaluation of the ZCSM method, which aims to improve CMM measurement accuracy of large complex optical surfaces.

The ZCSM method leverages Zernike polynomials to effectively solve the systematic geometric errors in CMM contact measurements. These errors often arise from probe deflection or misalignment during high-speed scanning. In this study, a PhaseCam 6000 interferometer was used as a high-precision reference to provide a benchmark for evaluating the accuracy of the ZCSM method. The method includes a Zernike fitting process to decompose the systematic geometric errors in CMM measurement by comparing Zernike coefficients of the WMI results. Systematic measurement errors are eliminated by subtracting relevant low-order aberrations in the Zernike polynomials.

The introduction of the DEC method is an important component of the ZCSM framework. It systematically corrects systematic geometric errors through iterative wavefront aberration correction and surface profile error evaluation. The linear BFS algorithm is essential to simplify aspheric surface fitting. It can evaluate surface profile errors based on the radius of curvature and dR, making the process more efficient and simpler.

Experimental results using an astronomical mirror with the 1429.5 mm-radius show that the accuracy of the ZCSM is comparable to that of the WMI method. The proposed method offers a wider dynamic range and greater flexibility in surface measurements, making it a viable alternative to conventional methods. The close alignment of the PV profile errors further supports the potential of the ZCSM approach for precision metrology of large optical surface in situations where interferometry is impractical.

Future research should focus on enhancing the applicability and accuracy of ZCSM by developing advanced feature

extraction and data alignment techniques to address angular offsets problem. Furthermore, improving the process for eliminating high-order background aberrations like coma or spherical aberration is essential to improve the accuracy of astigmatism measurement. Comparative studies benchmarking ZCSM against WMI with CGH measurements, especially for large free-form and aspheric surfaces, can help identify the unique advantages and limitations of each method.

Data availability statement

Data underlying the results presented in this paper are not publicly available at this time but may be obtained from the authors upon reasonable request.

Acknowledgment

We would like to thank the Shanghai Institute of Technical Physics (SITP) of the Chinese Academy of Sciences for their support.

ORCID iDs

Juliana Mei yuk Tam  <https://orcid.org/0000-0002-8581-5203>

Hester Chow  <https://orcid.org/0000-0001-7529-550X>

References

- [1] Ye J, Chen L, Li X, Yuan Q and Gao Z 2017 Review of optical freeform surface representation technique and its application *Proc. SPIE* **56** 110901
- [2] Gao Y, Cheng D, Xu C, Wang Y 2016 Design of an ultrashort throw catadioptric projection lens with a freeform mirror *Proc. SPIE* **10154** 101540S
- [3] Cheng D, Wang Y, Hua H and Talha M M 2009 Design of an optical see-through head-mounted display with a low f-number and large field of view using a freeform prism *Appl. Opt.* **48** 2655–68
- [4] Huang C K, Wu Y Q, Fan B, Yan F T, Liu F W, Zhang Y H 2014 A new method on measuring radius of curvature of a conic aspherical mirror *Proc. SPIE* **9280** 283–291
- [5] Fortmeier I, Stavridis M, Wiegmann A, Schulz M, Osten W and Elster C 2016 Evaluation of absolute form measurements using a tilted-wave interferometer *Opt. Express* **24** 3393–404
- [6] Liu Q, Li L, Zhang H, Huang W and Yue X 2020 Simultaneous dual-wavelength phase-shifting interferometry for surface topography measurement *Opt. Lasers Eng.* **124** 105813
- [7] Burge J H 1995 Applications of computer-generated holograms for interferometric measurement of large aspheric optics *Proc. SPIE* **2576** 258–69
- [8] Zhang X, Hu H, Xue D, Cheng Q, Yang X, Tang W, Qiao G and Zhang X 2023 Wavefront optical spacing of freeform surfaces and its measurement using CGH interferometry *Opt. Lasers Eng.* **161** 107350
- [9] Murphy P, Forbes G, Fleig J, Dumas P and Tricard M 2003 Stitching interferometry: a flexible solution for surface metrology *Opt. Photonics News* **14** 38–43
- [10] Peng J, Xu H, Yu Y and Chen M 2015 Stitching interferometry for cylindrical optics with large angular aperture *Meas. Sci. Technol.* **26** 25204–7
- [11] Aguirre-Aguirre D, Carrasco E, Izazaga-Pérez R, Páez G, Granados-Agustín F, Percino-Zacarías E, de Paz A G, Gallego J, Iglesias-Páramo J and Villalobos-Mendoza B 2018 MEGARA optics: sub-aperture stitching interferometry for large surfaces *Publ. Astron. Soc. Pac.* **30** 1–11
- [12] Chen S, Li S, Dai Y and Zheng Z 2007 Testing of large optical surfaces with subaperture stitching *Appl. Opt.* **46** 3504–9
- [13] Tam J M, Yu K M and Sun R L 2015 Integrated computer-aided verification of turbine blade *Comput.-Aided Des. Appl.* **12** 589–600
- [14] Zhu S, Wang D, Kang W and Liang R 2023 On-axis deflectometric system for freeform surface measurement *Opt. Lett.* **48** 1986–9
- [15] OLYMPUS Corporation 2018 LEXT OLS5000 3D measuring laser microscope brochure *OLYMPUS website*
- [16] Henselmans R, Cacace L A, Kramer G F Y, Rosielle P C J N and Steinbuch M 2011 The NANOMEFOS non-contact measurement machine for freeform optics *Precis. Eng.* **35** 607–24
- [17] Wu M, Han J, Hu W, Li M, Yang F and Sheng W 2022 Enhanced-spatial-resolution optical surface profiler based on focusing deflectometry *Opt. Express* **30** 45918–29
- [18] Sladek J 2016 *Coordinate Metrology : Accuracy of Systems and Measurements* (Springer)
- [19] Nouria H, Bergmans R H, Küng A, Piree H, Henselmans R and Spaan H A M 2014 Ultra high precision CMMs and their associated tactile or/and optical scanning probes *Int. J. Metrol. Qual. Eng.* **5** 204
- [20] Otto W et al 2000 Measuring large aspherics using a commercially available 3D-coordinate measuring machine *Proc. SPIE* **4003** 91–97
- [21] Wang X, Xian J, Yang Y, Zhang Y, Fu X and Kang M 2017 Use of coordinate measuring machine to measure circular aperture complex optical surface *Measurement* **100** 1–6
- [22] Taylor Hobson Ltd 2018 Form talysurf pgi optics surface profilometers brochure *Taylor Hobson website*
- [23] Yang P, Ye S and Peng Y 2017 Three-dimensional profile stitching measurement for large aspheric surface during grinding process with sub-micron accuracy *Precis. Eng.* **47** 62–71
- [24] Jing H, King C and Walker D 2010 Simulation and validation of a prototype swing arm profilometer for measuring extremely large telescope mirror-segments *Opt. Express* **18** 2036–48
- [25] Dong Z, Cheng H, Ye X and Tam H-Y 2014 Developing on-machine 3D profile measurement for deterministic fabrication of aspheric mirrors *Appl. Opt.* **53** 4997–5007
- [26] Li Y and Gu P 2005 Inspection of free-form shaped parts *Robot. Comput. Integr. Manuf.* **21** 421–30
- [27] Chen S, Dai Y, Peng X and Li S 2016 Error analysis and surface reconstruction for swing arm profilometry *Measurement* **87** 1–12
- [28] Lin X H, Wang Z Z, Guo Y B, Peng Y F and Hu C L 2014 Research on the error analysis and compensation for the precision grinding of large aspheric mirror surface *Int. J. Adv. Manuf. Technol.* **71** 233–9
- [29] Jin Y, Liao H and Pierson H 2019 Automatic feature-based point cloud alignment and inspection *25th Int. Conf. on Production Research Manufacturing Innovation: Cyber Physical Manufacturing* vol 39 pp 484–92

- [30] Wang S, Cheung C F, Ren M and Liu M 2018 Fiducial-aided robust positioning of optical freeform surfaces *Micromachines* **9** 52
- [31] Niu K and Tian C 2022 Zernike polynomials and their applications *J. Opt.* **24** 123001
- [32] ISO 10110-Part12 2007 Optics and Photonics—Preparation of Drawings for Optical Elements and Systems—Part 12: Aspheric Surfaces (International Organisation for Standardization)
- [33] Fortmeier I *et al* 2024 Results of round robin form measurements of optical aspheres and freeform surfaces *Meas. Sci. Technol.* **35** 85012
- [34] Minetola P 2012 The importance of a correct alignment in contactless inspection of additive manufactured parts *Int. J. Precis. Eng. Manuf.* **13** 211–8
- [35] Wang Z, Qu W and Asundi A 2017 A simplified expression for aspheric surface fitting *Optik* **140** 291–8